Zygote

cambridge.org/zyg

Cell cycle timing and centromere positioning in *Bos taurus* zygotes derived from *in vitro* fertilization

Federica Modafferi[1], Laura Thompson[2], Caitríona M. Collins[3], Elena O'Callaghan[2], Patrick Lonergan[2] and Elaine M. Dunleavy[1]

[1]Centre for Chromosome Biology, Biomedical Science Building, University of Galway, Galway, H91W2TY, Ireland; [2]Animal and Crop Sciences, School of Agriculture and Food Science, University College Dublin, Belfield, Dublin, D04 V1W8, Ireland and [3]Bioveterinary and Microbial Sciences, Technological University of the Shannon, Athlone Campus, University Road, Athlone, County Westmeath, N37 HD68, Ireland

Research Article

Cite this article: Modafferi F *et al*. (2025). Cell cycle timing and centromere positioning in *Bos taurus* zygotes derived from *in vitro* fertilization. *Zygote*. page 1 of 8. doi: 10.1017/S0967199425100221

Received: 27 February 2025
Revised: 14 July 2025
Accepted: 15 November 2025

Keywords:
Bovine IVF; cell cycle; centromere; chromosome; mitosis; S-phase

Corresponding author:
Elaine M Dunleavy; Email: elaine.dunleavy@universityofgalway.ie

Abstract

Centromeres are chromosomal loci essential for the correct segregation of genetic material during cell division. Defects in centromere function can lead to aneuploidy and cancer. During early embryonic development in mammals, prior to the first cell division, male and female genomes are separated in pronuclei located at the centre of the zygote. Parental chromatin clusters at the interface between the two pronuclei and this clustering step is critical to avoid aneuploidy in human and bovine zygotes. Yet, despite their essential function in chromosome segregation, the position and spatial organization of centromeres during the first cell cycle in mammals is mostly unknown. Previous studies conducted in bovine embryos derived from *in vitro* fertilization (IVF) showed that cell cycle progression impacts on the success rate of blastocyst formation. Specifically, embryos that entered earliest into S-phase or the earliest cleaving embryos were more likely to develop into blastocysts. To determine the precise timing of these events we performed a detailed characterization of key phases of the first cell cycle in bovine zygotes derived from IVF. In parallel we examined the spatial positioning of centromeres. We identify 20 h post insemination (hpi) as the timepoint when male and female pronuclei are juxtaposed and are completing S-phase. At this timepoint, we show that centromeres are positioned distal to the pronuclear interface and use super resolution microscopy to demonstrate extensive centromere clustering into chromocentres. Our results identify distinct nuclear features observed at 20 hpi, which may serve as cell cycle markers in determining successful bovine IVF.

Introduction

Centromeres are identified as the primary constriction of chromosomes and function in chromosome segregation during cell division. This is achieved via the assembly of a protein complex at the centromere, called the kinetochore, which serves as the platform for spindle microtubule attachment to pull chromosomes to opposite poles (Musacchio and Desai, 2017; Kixmoeller *et al.*, 2020). Active centromeres are specified by the incorporation of the histone H3 variant Centromere Protein A (CENP-A) that replaces histone H3 in a small percentage of centromeric nucleosomes (McKinley and Cheeseman, 2016). At the DNA level, centromeres are composed of repetitive DNA sequences called satellites. Satellite DNA is composed of repeated monomers assembled into higher order repeats (HORs). A portion of these HORs will be the sites at which CENP-A is enriched and where a functional kinetochore protein complex is assembled (Altemose *et al.*, 2022).

Defective centromere function has been implicated in cancer progression in mitotically dividing cells (Simeonova and Almouzni, 2024). In meiosis, defective chromosome segregation can result in aneuploid gametes or infertility, while aneuploidy in early development can result in embryo lethality (Potapova and Gorbsky, 2017; Charalambous *et al.*, 2023). In mammals, embryo development begins with the fertilization of the oocyte by the sperm. The genomes from sperm and oocyte are united to form a diploid cell, the zygote, that undergoes several rounds of mitosis to form the blastocyst (Molè *et al.*, 2020). Prior to the first mitotic division, before nuclear envelope breakdown, the male and female pronuclei are juxtaposed at the centre of the cell and chromatin clusters at the pronuclear interface (Cavazza *et al.*, 2021). In human and bovine embryos, clustering of the parental pronuclei is important for the correct segregation of chromosomes during the first mitotic division (Cavazza *et al.*, 2021). Despite the critical function of centromeres in faithful chromosome segregation, a detailed characterization of centromere dynamics during early embryogenesis is lacking in any mammal. Previous studies have focused on quantifying CENP-A levels across the early mitotic divisions in mouse embryos

(Das *et al.*, 2022; Manske *et al.*, 2022, pre-print) but the spatial organization in the cell cycle stages preceding the first mitotic division has not been described in detail. For instance, centromere clustering has been observed in various organisms and cell types and is proposed to maintain genome stability by preventing double strand breaks (Muller *et al.*, 2019). The position of the centromere in the different cell cycle phases could serve as a biomarker to select zygotes that are more likely to develop normally.

Studying early embryonic development in human embryos is challenging because of ethical regulations. *Bos taurus* (cattle) is an appropriate model system for human early development for several reasons. Bovine and human early embryos share a similar timing of early embryonic divisions (Lequarre *et al.*, 2003; Wong *et al.*, 2010; Faramarzi *et al.*, 2018), similar timing of zygotic genome activation (Frei *et al.*, 1989; Schulz and Harrison, 2019; Halstead *et al.*, 2020) and similar rates of aneuploidy (Destouni *et al.*, 2016). Moreover, in human and bovine embryos the first embryonic divisions happen in the presence of centrioles, which are inherited from the sperm (Navara *et al.*, 1994; Fishman *et al.*, 2018).

Investigating early embryogenesis in cattle is also beneficial to the agricultural industry. Reproductive efficiency is the cornerstone of all animal-based agricultural enterprises and is crucial for profitable, environmentally sustainable, food systems. In livestock production systems, particularly cattle production, reproductive efficiency is the main driver of farm profitability. Similar to humans, pregnancy loss, rather than fertilization failure, is one of the major causes of reproductive failure in cattle (Diskin and Morris, 2008; Wiltbank *et al.*, 2016) and can have a major impact on profitability due to costs associated with increased calving intervals, increased culling, increased labour costs and increased interventions of one form or another (Shalloo *et al.*, 2014). Such losses are exacerbated when *in vitro* produced embryos are used (Crowe *et al.*, 2025).

Currently, biomarkers predicting successful development to the blastocyst stage are lacking. In particular, the development of non-invasive nuclear and chromosomal factors to predict embryo viability are of interest (Sugimura *et al.*, 2024). Previous studies investigating the timing of bovine early embryonic divisions focused on the influence of semen quality and length of the first cell cycle on the blastocyst success rates. Researchers found that semen quality affects the timing of onset of the first S-phase. Zygotes originated by fertilization with high fertility semen started S-phase earlier than those fertilized with low fertility semen (Eid *et al.*, 1994; Comizzoli *et al.*, 2000). Additional studies highlighted a correlation between the timing of the first cleavage and the blastocyst success rate, with early cleaving zygotes more likely to develop into blastocysts (Lonergan *et al.*, 1999; Ward *et al.*, 2001). Notably, the timing of first cleavage is also used for embryo selection in human IVF (Shoukir *et al.*, 1997; Lechniak *et al.*, 2008; Sakkas, 2016). Also in humans, DNA replication stress in the first S-phase correlates with aneuploidy detected in subsequent mitotic divisions (Palmerola *et al.*, 2022), but it is not known whether this is the case in bovine zygotes. Finally, Lonergan et al. identified that the ability to reach blastocyst stage is heavily influenced by the time of first cleavage, but that once reached, pregnancy rates are similar after embryo transfer (Lonergan *et al.*, 1999). Therefore, timely progression through the first cell cycle is critical and additional biomarkers are needed. In this study, we aim to characterize in more detail the first mitoses after fertilization in *Bos taurus* zygotes derived from IVF. We focus on determining the cell cycle timing of S- and M-phases as well as centromere positioning.

Materials and methods

In vitro production of zygotes

Immature cumulus-oocyte complexes (COCs) were collected from the ovaries of heifers and cows following slaughter at a commercial abattoir. Ovaries were removed from the reproductive tract in the abattoir and stored in flasks of PBS at 35°C until arrival at the laboratory (approximately 3 h post slaughter). Once in the laboratory, all surface visible follicles were aspirated using a 5-mL syringe and 18-guage needle to recover the COCs. COCs were washed in phosphate-buffered saline and matured for 24 h in groups of 50 in 500 µL of IVM Medium (Stroebech Media) at 39°C under an atmosphere of 5% CO_2 in air with maximum humidity. Matured COCs with expanded cumulus cells were inseminated with frozen-thawed motile sperm at concentration 1×10^6 sperm/mL for 24 h from a bull of proven fertility. Under these conditions typically 80% of immature bovine COCs with expanded cumulus cells resume meiosis and progress to metaphase II (Lonergan and Fair, 2016; Ferré *et al.*, 2020). Gametes were co-incubated in groups of 50 in 400 µL of IVF Medium (Stroebech Media) at 39°C in an atmosphere of 5% CO_2 in air with maximum humidity. Presumptive zygotes were removed from culture at 3 ($n = 23$), 6 ($n = 32$), 9 ($n = 21$), 17 ($n = 23$), 20 ($n = 25$), 30 ($n = 25$) and 45 ($n = 19$) hours post insemination (hpi), gently vortexed in PBS to remove adherent cumulus cells and sperm before incubation with 5-ethynyl 2´-deoxyuridine (EdU) and fixation with 4% paraformaldehyde.

Generation of fluorescence in situ hybridization (FISH) probes

DNA FISH probes were generated by PCR from genomic DNA extracted from bull testes using the following primers based on Escudeiro *et al.*, 2019a: CenSAT1.723: F: 5'- CTGTGCTAGGG-AGCCCAAA -3', R: 5'- CAGGTTTGGAGCCCAATGCC -3'; SAT1.715 F1: 5'- AGGCTGCCTCTTGTGTTGGC -3', R1: 5'-CGTCGCAACTTGAGAATCCC -3'.

Cell biology: Combined 5-ethynyl 2´-deoxyuridine (EdU), FISH and immunofluorescence microscopy (IF) on zygotes

Zygotes at desired timepoints were incubated with EdU (Berry & Associates, PY7562) at 10 µM for 30 min and fixed in 4% paraformaldehyde for 30 min. EdU was visualized by click-chemistry in which a 200 µL reaction was assembled in 1X PBS with 40 mM $CuSO_4$ (Berry & Associates), 10 mM Na L-ascorbate (Berry & Associates) and 0.3 mM TEG-Azide conjugated with Alexa Fluor 647 (Invitrogen, A10277). After a 30-minute incubation in the dark, the samples were washed three times for 30 min each at room temperature in 1X PBS with 0.5% Triton-X-100 (PBST0.5). For FISH, samples were then dehydrated by passing through ethanol at 70%, 80% and 95% v/v for 5 min each. Zygotes were washed for 10 min in 2X SSC-Tween 20 (SSC-Tw) 0.1%, followed by a 10-minute wash in 2X SSC-Tw 0.1% with 25% formamide and a final wash for 10 min in 2X SSC-Tw 0.1% with 50% formamide. Pre-hybridization was carried out for 1 h at 37°C in 2X SSC-Tw 0.1% with 50% formamide. Probes were diluted in 100 µL hybridization buffer (0.2% Triton X-100 in 3X SSC, 50% formamide, 20% dextran sulphate) at a final concentration of 1 ng/µL. Denaturation was performed at 90°C for 10 min followed by hybridization overnight (o/n) at 37°C. Zygotes were washed once in 2X SSC-Tw 0.1% with 50% formamide for 1 h at 37°C followed by two washes in 2X SSC-Tw 0.1% with 25% formamide and 2X SSC-Tw 0.1% at room temperature for 10 min each. A final

https://doi.org/10.1017/S0967199425100221 Published online by Cambridge University Press

10-minute wash was performed in 1X PBS. Following FISH, samples were processed for immunofluorescence microscopy. Permeabilization was performed o/n at room temperature in PBST0.5, followed by blocking in Normal Goat Serum (NGS) 5% (prepared in PBST0.5). Primary antibody incubation was carried out o/n at 4°C with a rabbit anti-H3pSer10 antibody (Abcam, ab5176, 1:200 in NGS 1% in PBST0.1). Secondary antibody incubation was performed for 1 h at room temperature with a goat anti-rabbit secondary antibody conjugated with Alexa Fluor 488 (Invitrogen, A11034, 1:500 in NGS 1%). Three 20-minute washes in PBST0.4 were performed after each antibody incubation. Finally, DNA was stained with Hoechst (1:200 in 1X PBS) for 30 min and washed for 30 min in 1X PBS.

Microscopy

Zygotes were imaged using the Delta Vision Elite widefield microscope (Applied Precision, Imsol) using a 40x or 100x oil immersion objective, solid-state light source (Lumencor) and CoolSNAP_HQ2/HQ2-ICX285 camera. Fluorescence passed through a 435/48 nm; 525/48 nm; 597/45 nm; 632/34 nm band-pass filter for detection of respectively Hoechst, Alexa Fluor 488, Alex Fluor 546 and Alexa Fluor 647 in sequential mode. Z-stacks were performed with 0.1 µm thickness. After acquisition images were deconvolved with Softworx (Applied Precision, Imsol) and were processed using FIJI ImageJ (Rasband, 1997; Schneider *et al.*, 2012). Super resolution images were acquired using a Nikon CSU-W1 SoRa spinning disc system with 447/60nm; 525/50nm; 630/92nm filter sets and 405, 488 and 561 laser lines (Edinburgh Super-Resolution Imaging Consortium).

Quantitation and statistical analysis

The number of centromere foci at 20 and 30 hpi was measured in FIJI/ImageJ. Briefly, Z-stacks with centromere signals were max intensity projected, background was subtracted, a threshold was set to eliminate unwanted objects and the number of foci per nucleus was extracted. Histograms generated using GraphPad Prism 10 show the percentage of oocytes/zygotes at each timepoint as mean±SEM.

Results

To perform a detailed characterization of the timing of the first cell cycle in *Bos taurus*, a combination of EdU incorporation to mark S-phase and antibody staining for histone H3 phosphorylated at serine 10 (H3pSer10) to mark M-phase (meiosis or mitosis) was utilized. In parallel, to track the spatial position and organization of centromeres, we labelled centromeric DNA by FISH (Figure 1A). In *Bos taurus*, CENP-A is associated with the 680-base pair (bp) repeat SAT1.723 that defines the active centromere (Plucienniczak *et al.*, 1985; Escudeiro *et al.*, 2019a), which we refer to as CenSAT1.723. Presumptive zygotes and cleaved embryos derived from IVF were fixed at different timepoints after insemination. These timepoints included 3, 6, 9, 17, 20, 30 and 45 hpi. Before fixation, the presumptive zygotes were incubated with EdU for 30 min to pulse label ongoing DNA synthesis. After fixation, EdU signal was visualized by performing the click chemistry reaction, followed by FISH labelling of centromeric DNA and immunofluorescent staining of condensed chromosomes (Figure 1A). Quantitation of cells in meiosis, S- or M-phases indicated that almost 100% of zygotes are in meiosis up to 9 hpi and most zygotes are in S-phase at 17 hpi (72%) and 20 hpi (93%). Most zygotes complete the first mitosis by 30 hpi (78%) to give rise to 2-cell embryos and complete the second mitosis at 45 hpi (68%) to give rise to 4-cell embryos (Figure 1B).

At 6 hpi and 9 hpi, approximately 80% of oocytes are completing meiosis II after which the second polar body is extruded and the nucleus is positioned close to the cellular periphery (Figure 2A). H3pSer10 stains condensed chromosomes that are commonly arranged in a ring shape and centromeres are visible as chromosomally associated foci (Figure 2B). We noted that chromosomes localized at the centre of the ring did not stain for H3pSer10 possibly due to enhanced chromosome condensation and a lack of antibody penetration in this region. The decondensing sperm nucleus is normally visible during this time window; however, it was undetectable in our experiments due to interference of the click chemistry reaction with DNA staining. Remaining cumulus cells of the COC also stained positive for CenSAT1.723 showing the typical pattern expected for centromere foci in somatic cells (Figure 2A).

At 17 hpi (Figure 3A, 3B) and 20 hpi (Figure 3C, 3D), the two pronuclei are undergoing DNA replication in S-phase. At 17 hpi, zygotes are in early/mid S-phase displaying the typical distribution pattern for EdU that is spread throughout the nucleus (O'Keefe *et al.*, 1992). Entry into S-phase is asynchronous, with either only one of the parental nuclei displaying EdU positive signals or with each pronucleus displaying a different pattern indicating a different stage of early/mid-S-phase. At this timepoint, centromeres are clustered at the centre of each pronucleus. At 20 hpi, pronuclei migrate to the centre of the cell and are in opposition, displaying weak and sparse EdU foci likely indicative of late S-phase (Figure 3D). This timepoint corresponds with the previously described stage of chromatin clustering at the pronuclear interface that occurs approximately 1.5 h before nuclear membrane breakdown (Cavazza *et al.*, 2021). At this timepoint, centromeres are located away from the pronuclear interface or are in a more central position. Further quantitation of centromere spatial positioning indicated that in most zygotes (85.7%, $n = 14$) centromeres were located distal to the pronuclear interface where the centrosomes that emanate microtubules and capture centromeres normally reside. We also show evidence for centromere clustering at 20 hpi, in which 22.0 ± 1.44 centromere foci per nucleus were detected ($n = 41$) instead of 30 expected for the haploid bovine karyotype.

To investigate this localization pattern at 20 hpi in more detail, in addition to CenSAT1.723, we used FISH probes to label the pericentromeric satellite SAT1.715 composed of 31-bp variable monomers that assemble into a 1402 bp HOR (Płucienniczak *et al.*, 1982; Escudeiro *et al.*, 2019a, 2019b). We combined FISH with DNA staining to monitor chromatin clustering at the pronuclear interface and imaged the zygotes using super resolution microscopy (Figure 4A). Super resolution imaging of pronuclei confirmed that, based on the CenSAT1.723 staining pattern, centromeres are not positioned at the pronuclear interface but instead are distributed in clusters throughout both pronuclei. We also observed that centromeres cluster into distinct chromocentres, with circular or layered organizations (Figure 4B). In contrast, based on the SAT1.715 pattern, pericentromeric DNA is not organized into clusters and extends throughout both pronuclei, occupying a large portion of each pronucleus.

At 30 hpi (Figure 5A), zygotes complete chromosome segregation in mitosis and the first cleavage has occurred to generate a 2-cell embryo. At this timepoint, both cells have entered S-phase although this is usually not synchronous (Figure 5B).

https://doi.org/10.1017/S0967199425100221 Published online by Cambridge University Press

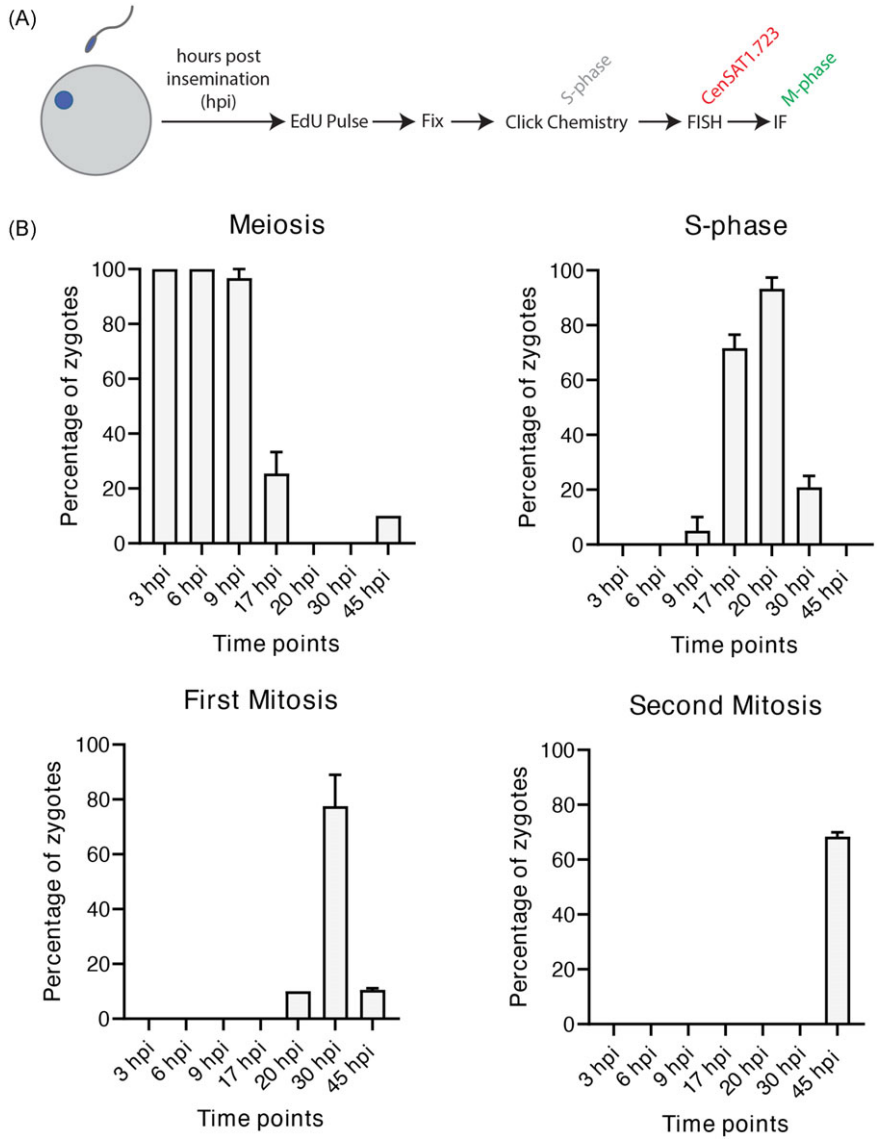

Figure 1. Timing of the first cell cycle in *Bos taurus* zygotes from IVF. (A) Schematic of the EdU, FISH, IF protocol. After IVF, the zygotes were incubated with EdU for 30 min, fixed at the desired timepoints and processed further for FISH and IF. (B) Quantitation of zygotes at the different cell cycle stages assigned by observing the EdU and H3pSer10 signals. H3pSer10 labelling of condensing chromosomes was classified as meiosis or mitosis. In 17 and 20 hpi zygotes, S-phase was assigned if at least one of the pronuclei showed EdU incorporation. Percentage of zygotes in other cell cycle stages (*e.g.* G1, G2 and 8-/16-cell embryos) is not shown. Results are expressed as mean±SEM. 3 hpi, $n = 23$ zygotes; 6 hpi, $n = 32$ zygotes; 9 hpi, $n = 21$ zygotes; 17 hpi, $n = 23$ zygotes; 20 hpi, $n = 25$ zygotes; 30 hpi, $n = 25$ zygotes, 45 hpi, $n = 19$ zygotes.

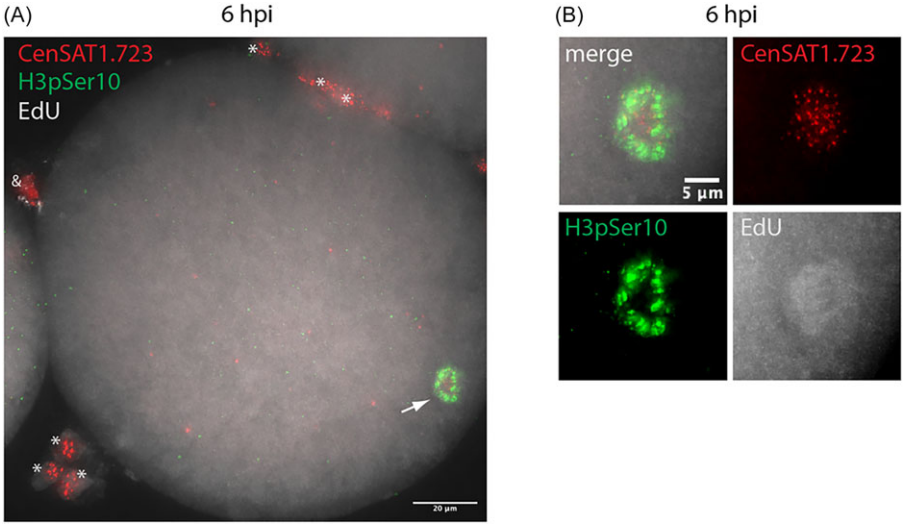

Figure 2. The *Bos taurus* oocyte is completing meiosis up to 9 h post insemination. (A) 40x image of a 6 hpi zygote in prometaphase of meiosis I or II. The nucleus is indicated by the white arrow. Scale bar, 20 µm. The polar bodies are not visible. Therefore, it is not possible to distinguish between meiosis I and II. *CenSAT1.723 staining of cumulus cells; cells in the upper part of the image appear flat as they are sandwiched between two oocytes. [&]Non-specific probe binding. (B) Magnification of the nucleus indicated with the arrow in A. Scale bar, 5 µm. In both A and B, H3pSer10 (green) marks condensed chromosomes in meiosis, CenSAT1.723 (red) DNA FISH probe labels centromeres and EdU (grey) marks DNA replication in S-phase. hpi, hours post insemination; H3pSer10, H3 phosphorylated at serine 10.

https://doi.org/10.1017/S0967199425100221 Published online by Cambridge University Press

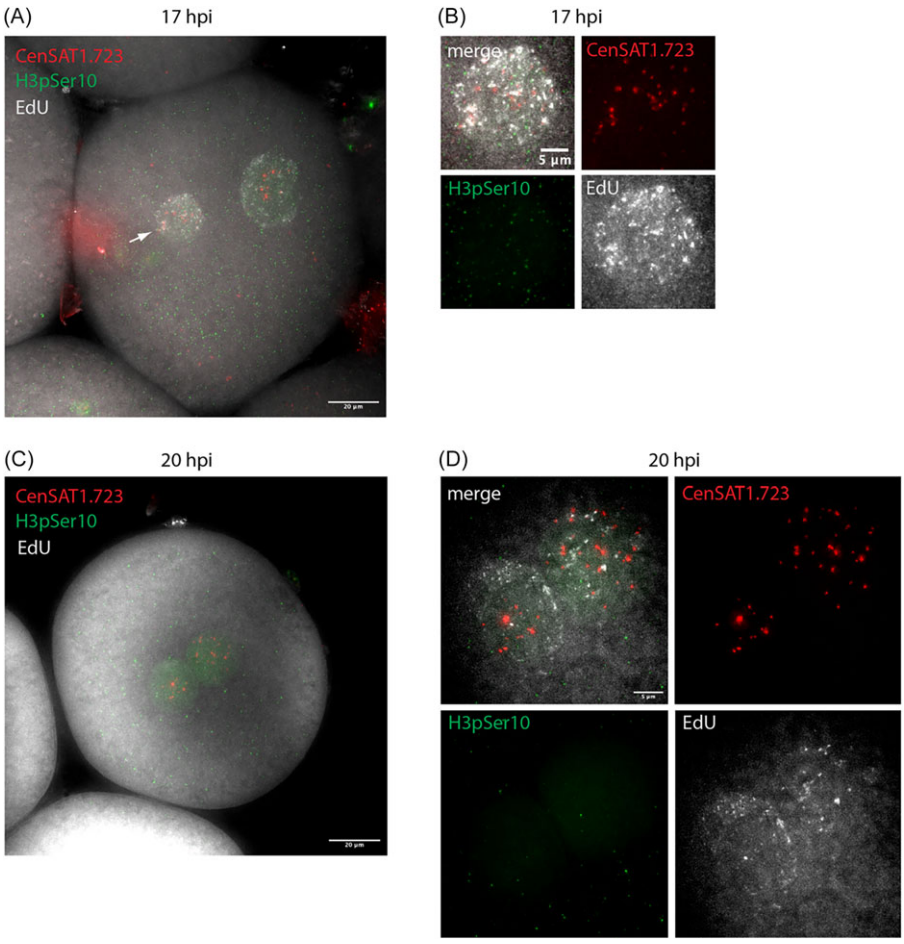

Figure 3. At 17 and 20 hpi, *Bos taurus* pronuclei are in S-phase. (A) 40x image of a zygote at 17 hpi. The parental pronuclei are visible and they are positive for EdU. Scale bar, 20 µm. (B) Magnification of the pronucleus indicated by the arrow in A. Scale bar, 5 µm. (C) 40x image of a zygote at 20 hpi. At this stage the two pronuclei are juxtaposed and are completing S-phase. Scale bar, 20 µm. (D) 100x image of pronuclei in C with EdU signal enhanced to show weak foci. Scale bar, 5 µm. H3pSer10 is shown in green, CenSAT1.723 in red and EdU in grey. hpi, hours post insemination; H3pSer10, H3 phosphorylated at serine 10.

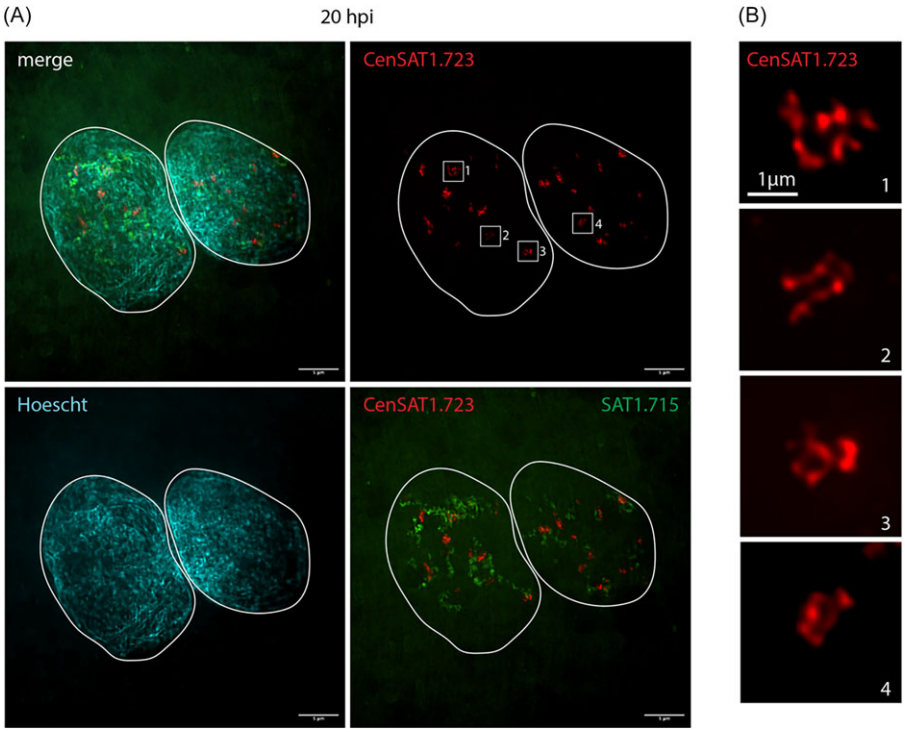

Figure 4. At 20 hpi, *Bos taurus* centromeres are positioned distal to the pronuclear interface and form chromocentres. (A) Super resolution microscopy imaging of the parental pronuclei (circled) at 20 hpi. Scale bar 5 µm. (B) Magnification of the boxes highlighted in A. Individual centromeres are organized as chromocentres with a circular (boxes 1 and 3) or layered organization (boxes 2 and 4). Scale bar, 1 µm. Hoechst (cyan) labels the DNA, SAT1.715 DNA FISH probe (green) labels pericentromeric DNA and CenSAT1.723 (red) labels centromere DNA. hpi, hours post insemination.

https://doi.org/10.1017/S0967199425100221 Published online by Cambridge University Press

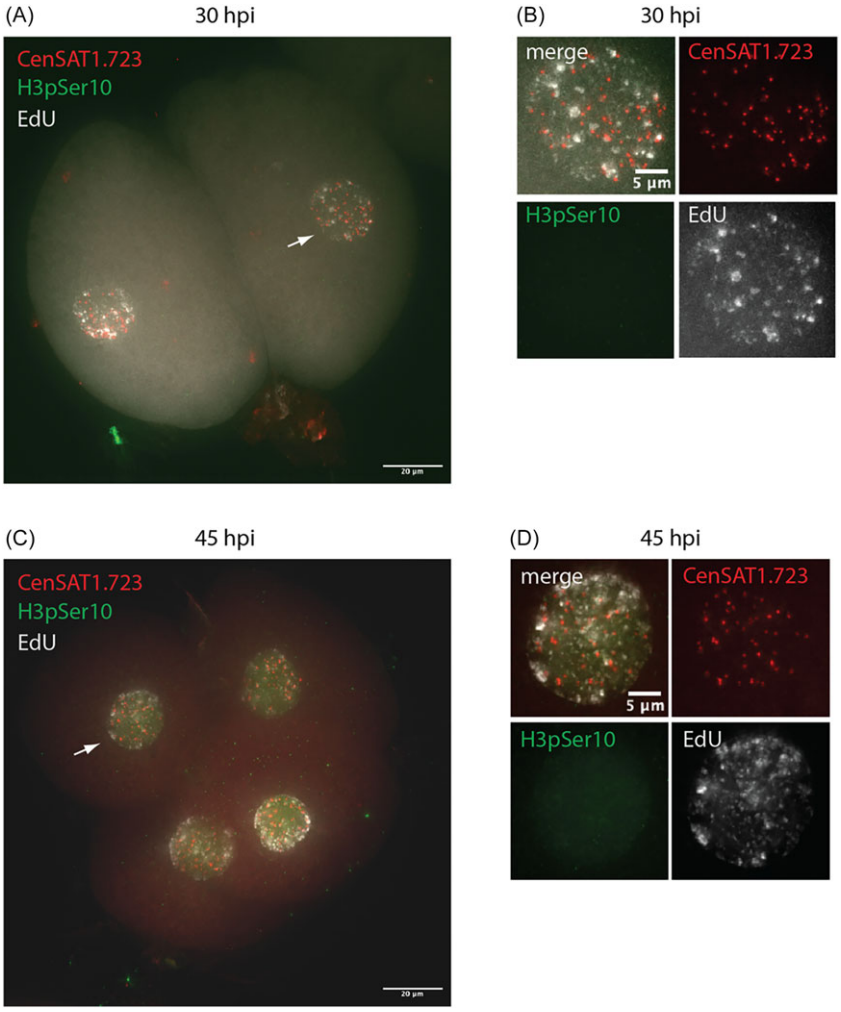

Figure 5. The first two mitotic divisions in *Bos taurus* embryos from IVF. (A) 40x image of a 2-cell embryo at 30 hpi. Both nuclei are undergoing DNA replication, although asynchronously. Scale bar, 20 µm. (B) Magnification of the nucleus indicated by the arrow in A. Scale bar, 5 µm. (C) 40x image of a 4-cell embryo at 45 hpi, after completion of the second mitotic division. Scale bar, 20 µm. (D) Magnification of the nucleus indicated by the arrow in C. Scale bar, 5 µm. H3pSer10 is in green, centromeric (CenSAT1.723) DNA in red and EdU in grey. hpi, hours post insemination; H3pSer10, H3 phosphorylated at serine 10.

Typically, 49 (±3.341) centromere foci per nucleus were detected ($n = 29$ nuclei), which is lower than the number expected based on bovine karyotype ($2n = 60$). This indicates that centromere clustering continues after cell division, comparable to the distinct chromocentres observed by super resolution at 20 hpi. At 45 hpi (Figure 5C), embryos are at the 4-cell stage and have completed the second mitotic division. At this timepoint, each cell is undergoing S-phase in an asynchronous manner and centromeres are broadly dispersed throughout the nuclei (Figure 5D).

Discussion

In the late 1980's, the ultrastructure of bovine oocyte maturation and in vitro fertilization (IVF) were first characterized (Hyttel *et al.*, 1988, 1989a, 1989b). Cell cycle studies performed in the 1990's later indicated that the duration and timing of S- and M-phases of the first cell cycle impacts on the success rate of blastocyst formation (Eid *et al.*, 1994; Lonergan *et al.*, 1999; Comizzoli *et al.*, 2000; Ward *et al.*, 2001). More recently, the juxtaposition of parental pronuclei with chromatin clustered at the pronuclear interface was identified as a critical step to avoid bovine embryos with abnormal chromosome numbers (Cavazza *et al.*, 2021). Using bovine zygotes fixed at different timepoints after IVF, we labelled S- and M-phase progression and determined centromere positioning at each stage. Our results show that the first S-phase in male and female pronuclei takes place at 17 and 20 hpi and the first M-phase takes place at 30 hpi. These data could be used in future studies to identify cell cycle delays that impact on blastocyst formation rate.

At 20 hpi, male and female pronuclei were juxtaposed and were in late S-phase. We also observed the clustering of chromatin at the pronuclear interface at this time, consistent with published data (Cavazza *et al.*, 2021). In this previous study, the timing of this event was determined as 1.5 h before nuclear breakdown based on time-lapse imaging approaches. Here we show that these nuclei are completing DNA replication at this timepoint. Also, at 20 hpi, we found that centromeres were located away from the pronuclear interface. This result is surprising given that centrosomes are located at the pronuclear interface and suggests a rapid relocalization occurs to enable efficient chromosome capture before the first mitosis. Close examination of the EdU incorporation patterns revealed that entry into S-phase is asynchronous between male and female pronuclei at 17 and 20 hpi. Furthermore, S-phase progression at 30 and 45 hpi is asynchronous in 2-cell and 4-cell embryos. It is not known whether this asynchrony occurs upon natural fertilization or is related to the IVF protocol. Our results highlighting 20 hpi as a critical timepoint align with findings related to the fidelity of the first embryonic S-phase in humans. Palmerola and colleagues showed that incomplete replication results in DNA double strand breaks in mitosis that

https://doi.org/10.1017/S0967199425100221 Published online by Cambridge University Press

impact the normal development of the embryo (Palmerola *et al.*, 2022). Future studies into the occurrence of DNA breaks in bovine zygotes at 20 hpi and identifying a correlation with blastocyst progression would be of interest. In conclusion, our study identifies the completion of S-phase at 20 hpi as a potentially useful timepoint and nuclear marker in the evaluation of early cleavage and the efficient prediction of embryo viability.

Funding. This work was supported by Research Ireland Grants 20/FFP-A/8519, GOIPG/2020/1113 and 16/IA/4474.

Competing interests. Authors declare no conflicts of interest.

Ethical standards. All experimental procedures involving animals were sanctioned by the Animal Research Ethics Committee of University College Dublin and were licensed by the Health Products Regulatory Authority, Ireland, in accordance with Statutory Instrument No.543 of 2012 under Directive 2010/63/EU on the Protection of Animals used for Scientific Purposes.

References

Altemose, N., Logsdon, G.A., Bzikadze, A.V., Sidhwani, P., Langley, S.A., Caldas, G.V., Hoyt, S.J., Uralsky, L., Ryabov, F.D., Shew, C.J., Sauria, M.E.G., Borchers, M., Gershman, A., Mikheenko, A., Shepelev, V.A., Dvorkina, T., Kunyavskaya, O., Vollger, M.R., Rhie, A., McCartney, A.M., Asri, M., Lorig-Roach, R., Shafin, K., Lucas, J.K., Aganezov, S., Olson, D., de Lima, L.G., Potapova, T., Hartley, G.A., Haukness, M., Kerpedjiev, P., Gusev, F., Tigyi, K., Brooks, S., Young, A., Nurk, S., Koren, S., Salama, S.R., Paten, B., Rogaev, E.I., Streets, A., Karpen, G.H., Dernburg, A.F., Sullivan, B.A., Straight, A.F., Wheeler, T.J., Gerton, J.L., Eichler, E.E., Phillippy, A.M., Timp, W., Dennis, M.Y., O'Neill, R.J., Zook, J.M., Schatz, M.C., Pevzner, P.A., Diekhans, M., Langley, C.H., Alexandrov, I.A. and Miga, K.H., (2022) Complete genomic and epigenetic maps of human centromeres. *Science* **376**, eabl4178. https://doi.org/10.1126/science.abl4178

Cavazza, T., Takeda, Y., Politi, A.Z., Aushev, M., Aldag, P., Baker, C., Choudhary, M., Bucevičius, J., Lukinavičius, G., Elder, K., Blayney, M., Lucas-Hahn, A., Niemann, H., Herbert, M. and Schuh, M., (2021) Parental genome unification is highly error-prone in mammalian embryos. *Cell* **184**(11), 2860–2877.e22. https://doi.org/10.1016/j.cell.2021.04.013

Charalambous, C., Webster, A. and Schuh, M., (2023) Aneuploidy in mammalian oocytes and the impact of maternal ageing. *Nature Reviews Molecular Cell Biology* **24**, 27–44. https://doi.org/10.1038/s41580-022-00517-3

Comizzoli, P., Marquant-Le Guienne, B., Heyman, Y. and Renard, J.P., (2000) Onset of the first S-phase is determined by a paternal effect during the G1-phase in bovine zygotes. *Biology of Reproduction* **62**, 1677–1684. https://doi.org/10.1095/biolreprod62.6.1677

Crowe, A.D., Sánchez, J.M., Moore, S.G., McDonald, M., McCabe, M.S., Randi, F., Lonergan, P. and Butler, S.T., (2025) Incidence and timing of pregnancy loss following timed artificial insemination or timed embryo transfer with a fresh or frozen in vitro-produced embryo. *Journal of Dairy Science* **108**, 1022–1038. https://doi.org/10.3168/jds.2024-25139

Das, A., Iwata-Otsubo, A., Destouni, A., Dawicki-McKenna, J.M., Boese, K.G., Black, B.E. and Lampson, M.A., (2022) Epigenetic, genetic and maternal effects enable stable centromere inheritance. *Nature Cell Biology* **24**, 748–756. https://doi.org/10.1038/s41556-022-00897-w

Destouni, A., Esteki, M.Z., Catteeuw, M., Tšuiko, O., Dimitriadou, E., Smits, K., Kurg, A., Salumets, A., Soom, A.V., Voet, T. and Vermeesch, J.R., (2016) Zygotes segregate entire parental genomes in distinct blastomere lineages causing cleavage-stage chimerism and mixoploidy. *Genome Research* **26**, 567–578. https://doi.org/10.1101/gr.200527.115

Diskin, M. and Morris, D., (2008) Embryonic and early foetal losses in cattle and other ruminants. *Reproduction in Domestic Animals* **43**, 260–267. https://doi.org/10.1111/j.1439-0531.2008.01171.x

Eid, L.N., Lorton, S.P. and Parrish, J.J., (1994) Paternal influence on S-phase in the first cell cycle of the bovine embryo1. *Biology of Reproduction* **51**, 1232–1237. https://doi.org/10.1095/biolreprod51.6.1232

Escudeiro, A., Adega, F., Robinson, T.J., Heslop-Harrison, J.S. and Chaves, R., (2019a) Conservation, divergence and functions of centromeric satellite DNA families in the bovidae. *Genome Biology and Evolution* **11**, 1152–1165. https://doi.org/10.1093/gbe/evz061

Escudeiro, A., Ferreira, D., Mendes-da-Silva, A., Heslop-Harrison, J.S., Adega, F. and Chaves, R., (2019b) Bovine satellite DNAs – a history of the evolution of complexity and its impact in the Bovidae family. *The European Zoological Journal* **86**, 20–37. https://doi.org/10.1080/24750263.2018.1558294

Faramarzi, A., Khalili, M.A., Omidi, M., Agha-Rahimi, A. and Taheri, F., (2018) Pronuclear pattern does not predict morphokinetics behavior in human embryos. *Gynecological Endocrinology* **34**, 248–251. https://doi.org/10.1080/09513590.2017.1388365

Ferré, L.B., Kjelland, M.E., Strøbech, L.B., Hyttel, P., Mermillod, P. and Ross, P.J., (2020) Review: recent advances in bovine *in vitro* embryo production: reproductive biotechnology history and methods. *Animal* **14**, 991–1004. https://doi.org/10.1017/S1751731119002775

Fishman, E.L., Jo, K., Nguyen, Q.P.H., Kong, D., Royfman, R., Cekic, A.R., Khanal, S., Miller, A.L., Simerly, C., Schatten, G., Loncarek, J., Mennella, V. and Avidor-Reiss, T., (2018) A novel atypical sperm centriole is functional during human fertilization. *Nature Communications* **9**, 2210. https://doi.org/10.1038/s41467-018-04678-8

Frei, R.E., Schultz, G.A. and Church, R.B., (1989) Qualitative and quantitative changes in protein synthesis occur at the 8–16-cell stage of embryogenesis in the cow. *Reproduction* **86**, 637–641. https://doi.org/10.1530/jrf.0.0860637

Halstead, M.M., Ma, X., Zhou, C., Schultz, R.M. and Ross, P.J., (2020) Chromatin remodeling in bovine embryos indicates species-specific regulation of genome activation. *Nature Communications* **11**, 4654. https://doi.org/10.1038/s41467-020-18508-3

Hyttel, P., Callesen, H. and Greve, T., (1989a) A comparative ultrastructural study of in vivo versus in vitro fertilization of bovine oocytes. *Anatomy and Embryology(Berl.)* **179**, 435–442. https://doi.org/10.1007/BF00319585

Hyttel, P., Greve, T. and Callesen, H., (1989b) Ultrastructural aspects of oocyte maturation and fertilization in cattle. *Journal of Reproduction and Fertility. Supplement* **38**, 35–47.

Hyttel, P., Xu, K.P. and Greve, T., (1988) Ultrastructural abnormalities of in vitro fertilization of in vitro matured bovine oocytes. *Anatomy and Embryology(Berl.)* **178**, 47–52. https://doi.org/10.1007/BF00305013

Kixmoeller, K., Allu, P.K. and Black, B.E., (2020) The centromere comes into focus: from CENP-A nucleosomes to kinetochore connections with the spindle. *Open Biology* **10**, 200051. https://doi.org/10.1098/rsob.200051

Lechniak, D., Pers-Kamczyc, E. and Pawlak, P., (2008) Timing of the first zygotic cleavage as a marker of developmental potential of mammalian embryos. *Reproductive Biology* **8**, 23–42. https://doi.org/10.1016/S1642-431X(12)60002-3

Lequarre, A.S., Marchandise, J., Moreau, B., Massip, A. and Donnay, I., (2003) Cell cycle duration at the time of maternal zygotic transition for in vitro produced bovine embryos: effect of oxygen tension and transcription inhibition1. *Biology of Reproduction* **69**, 1707–1713. https://doi.org/10.1095/biolreprod.103.017178

Lonergan, P. and Fair, T., (2016) Maturation of oocytes in Vitro. *Annual Review of Animal Biosciences* **4**, 255–268. https://doi.org/10.1146/annurev-animal-022114-110822

Lonergan, P., Khatir, H., Piumi, F., Rieger, D., Humblot, P. and Boland, M.P., (1999) Effect of time interval from insemination to first cleavage on the developmental characteristics, sex ratio and pregnancy rate after transfer of bovine embryos. *Reproduction* **117**, 159–167. https://doi.org/10.1530/jrf.0.1170159

Manske, G., Jorgensen, K., Ma, B., Aboelenain, M., Tower, C., Chakraborty, S., Ranjan, R., Das, A., Lampson, M.A., Black, B.E., Schindler, K., Chen, X. and Hammoud, S.S., (2022) Equalizing epigenetically imprinted centromeres in early mammalian embryos. https://doi.org/10.1101/2022.10.27.514094

McKinley, K.L. and Cheeseman, I.M., (2016) The molecular basis for centromere identity and function. *Nature Reviews Molecular Cell Biology* **17**, 16–29. https://doi.org/10.1038/nrm.2015.5

Molè, M.A., Weberling, A. and Zernicka-Goetz, M., (2020) Comparative analysis of human and mouse development: From zygote to pre-gastrulation, In Solnica-Krezel, L. (ed.), *Current Topics in Developmental Biology, Gastrulation: From Embryonic Pattern to Form*. Academic Press, pp. 113–138. https://doi.org/10.1016/bs.ctdb.2019.10.002

Muller, H., Gil, J. and Drinnenberg, I.A., (2019) The impact of centromeres on spatial genome architecture. *Trends in Genetics* **35**, 565–578. https://doi.org/10.1016/j.tig.2019.05.003

Musacchio, A. and Desai, A., 2017) A molecular view of kinetochore assembly and function. *Biology* **6**, 5. https://doi.org/10.3390/biology6010005

Navara, C.S., First, N.L. and Schatten, G., (1994) Microtubule organization in the cow during fertilization, polyspermy, parthenogenesis and nuclear transfer: the role of the sperm aster. *Developmental Biology* **162**, 29–40. https://doi.org/10.1006/dbio.1994.1064

O'Keefe, R.T., Henderson, S.C. and Spector, D.L., (1992) Dynamic organization of DNA replication in mammalian cell nuclei: spatially and temporally defined replication of chromosome-specific alpha-satellite DNA sequences. *The Journal of Cell Biology* **116**, 1095–1110. https://doi.org/10.1083/jcb.116.5.1095

Palmerola, K.L., Amrane, S., De Los Angeles, A., Xu, S., Wang, N., de Pinho, J., Zuccaro, M.V., Taglialatela, A., Massey, D.J., Turocy, J., Robles, A., Subbiah, A., Prosser, B., Lobo, R., Ciccia, A., Koren, A., Baslan, T. and Egli, D., (2022) Replication stress impairs chromosome segregation and preimplantation development in human embryos. *Cell* **185**, 2988–3007.e20. https://doi.org/10.1016/j.cell.2022.06.028

Płucienniczak, A., Skowroński, J. and Jaworski, J., (1982) Nucleotide sequence of bovine 1.715 satellite DNA and its relation to other bovine satellite sequences. *Journal of Molecular Biology* **158**, 293–304. https://doi.org/10.1016/0022-2836(82)90434-X

Plucienniczak, G., Skowronski, J., Plucienniczak, A. and Jaworski, J., (1985) Nucleotide Sequence of Bovine 1.723 Satellite DNA. *Zeitschrift für Naturforschung C* **40**, 242–246. https://doi.org/10.1515/znc-1985-3-418

Potapova, T. and Gorbsky, G.J., (2017) The consequences of chromosome segregation errors in mitosis and meiosis. *Biology* **6**, 12. https://doi.org/10.3390/biology6010012

Rasband, W.S., (1997) ImageJ, U.S. National Institutes of Health. Httprsbinfonihgovij 1997-2007.

Sakkas, D., (2016) Cleavage in the preimplantation embryo: it is all about being in the right place at the right time! *Molecular Human Reproduction* **22**, 679–680. https://doi.org/10.1093/molehr/gaw058

Schneider, C.A., Rasband, W.S. and Eliceiri, K.W., (2012) NIH Image to ImageJ: 25 years of image analysis. *Nature Methods* **9**, 671–675. https://doi.org/10.1038/nmeth.2089

Schulz, K.N. and Harrison, M.M., (2019) Mechanisms regulating zygotic genome activation. *Nature Reviews Genetics* **20**, 221–234. https://doi.org/10.1038/s41576-018-0087-x

Shalloo, L., Cromie, A. and McHugh, N., (2014) Effect of fertility on the economics of pasture-based dairy systems. *Animal* **8**, 222–231. https://doi.org/10.1017/S1751731114000615

Shoukir, Y., Campana, A., Farley, T. and Sakkas, D., (1997) Early cleavage of in-vitro fertilized human embryos to the 2-cell stage: a novel indicator of embryo quality and viability. *Human Reproduction (Oxford, England)* **12**, 1531–1536. https://doi.org/10.1093/humrep/12.7.1531

Simeonova, I. and Almouzni, G., (2024) Histone H3 Variants in the Multiverse of Cancer. *Annual Review of Cancer Biology* **8**, 453–474. https://doi.org/10.1146/annurev-cancerbio-062722-021823

Sugimura, S., Yao, T., Matoba, S., Yamagata, K. and Imai, K., (2024) Morphokinetic prediction of embryo viability in cattle. *Reproduction, Fertility and Development* **37**(1), RD24139. https://doi.org/10.1071/RD24139

Ward, F., Rizos, D., Corridan, D., Quinn, K., Boland, M. and Lonergan, P., (2001) Paternal influence on the time of first embryonic cleavage post insemination and the implications for subsequent bovine embryo development in vitro and fertility in vivo. *Molecular Reproduction and Development* **60**, 47–55. https://doi.org/10.1002/mrd.1060

Wiltbank, M.C., Baez, G.M., Garcia-Guerra, A., Toledo, M.Z., Monteiro, P.L.J., Melo, L.F., Ochoa, J.C., Santos, J.E.P. and Sartori, R., (2016) Pivotal periods for pregnancy loss during the first trimester of gestation in lactating dairy cows. Theriogenology, Proceedings of the 18th ICAR 86, 239–253. https://doi.org/10.1016/j.theriogenology.2016.04.037

Wong, C.C., Loewke, K.E., Bossert, N.L., Behr, B., De Jonge, C.J., Baer, T.M. and Pera, R.A.R., (2010) Non-invasive imaging of human embryos before embryonic genome activation predicts development to the blastocyst stage. *Nature Biotechnology* **28**, 1115–1121. https://doi.org/10.1038/nbt.1686

https://doi.org/10.1017/S0967199425100221 Published online by Cambridge University Press